REGULAR SHAPES DETECTION IN SATELLITE IMAGES

Ahmad R. Eskandari[1], Zahra Kouchaki [2]
[1] Digital Media Lab, AICTC Research Center,
Department of Computer Engineering, Sharif University of Technology, Tehran, Iran.
eskandari@dml.ir
[2] Department of Biomedical Engineering,
Science and Research Branch, Islamic Azad University, Tehran, Iran.
parisakouchaki@gmail.com

ABSTRACT

This paper presents a novel and fast method to distinguish regular and irregular regions in satellite and aerial images. This can be employed in further processing such as detecting man-made or artificial structures, disaster response, road sign detection and etc. In order to achieve this goal, we offer a suitable definition of regular shapes. Using this definition, we propose an appropriate technique to evaluate regularity .In our approach, discrete Fourier transform plays the main role for searching the regularity. We suggest a criterion; called RCNR, which indicates to some extent that the shape is regular. The computed RCNR value should be compared with a pre-assigned threshold value for making decision. Our suggested method has a good robustness against rotation and scale variation and could be easily implemented. Moreover, our approach is independent of the shape and has a low processing time. The experimental results show the capability and feasibility of the proposed technique in the classification of regions into regular and irregular shapes in satellite images.

Keywords: *Regular Shape Detection, Regular Shape Definition, RCNR, Remote Sensing, Man-made Detection.*

1.0 INTRODUCTION

Nowadays, along with the progression of extraction and easy access to information, the processing of satellite images has been perceived as one of the first priorities by the researchers in the field of Pattern Recognition and Computer Vision. There are many significant applications when discussing the processing of satellite and aerial images. One of the important processing issue is the classification of regions into regular and irregular forms which has many advantages in the fields such as geology, national development, military purposes, mapping, environmental monitoring, road sign detection system, disaster response, and etc.

Several methods have been proposed for inspecting regularity in the recent years. Piccioli et al. [1] retrieved triangular and square contours in an edge image by selecting the edge segments with proper slopes and checking whether their endpoints are close enough to form certain angles. This approach usually suffers difficulties when retrieving broken edges. Loy and Barnes [2] applied the radial symmetry algorithm to detect regular polygons. They took advantage of the radial symmetry nature of a regular polygon to locate its center. This method has high computational complexity for multi-shape detection, and also, is only dealing with polygon shapes. Moreover, Loy and Barnes's algorithm relies on edge detection algorithms that make it vulnerable to noise. Escaleera et al. [3] located triangular shapes by seeking the coexistence of three types of corners that form a triangle; and the similar principle was applied to square and circle detection. However, this method strongly relies on corner detection and classification, which is not robust in cluttered scenes such as satellite images. Gang wu et al. [4] presented a method to cope with this problem, but in his proposed method the regularity just defined in polygons and circle and also their algorithm, like loy Barnes's approach [2], relies on edge detection algorithms that make it non-robust against noisy shapes. Moreover, it is not optimal for classification between regular and irregular shapes due to the extra processing time for identification of the polygons.

In this work, we first present a suitable definition for regular shapes in satellite images which contain most of our objects of interest. Then, we specify some of the characteristics of regular shapes based on our definition and represent a suitable technique to research these characteristics on a shape and finally distinguish whether it is regular or not.

The rest of this paper contains: our definition of regular shapes in section 2, the steps of the proposed regular shape detection in details are presented in section 3 which consists of the complete explanation of our method. And finally, experimental results and the conclusion are set in section 4 and 5, respectively.

2.0 REGULAR SHAPES DEFINITION

In the concept of machine vision there is not an explicit definition of regular shapes. It is true that the definition is relative and depends on the application and the shapes we are working with. By inspecting satellite images, we conclude that most regular shapes are rectangular, square or circle. This conclusion is predictable because we know that most regular shapes in satellite images consist of artificial objects which are man-made structures. We present a definition for regular shapes that encompasses the three shapes mentioned above*: A shape is defined as regular if the whole shape is formed by a repetition of a particular part, in the same direction, at the sides of a regular polygon or by the repetition of this part, in the same direction, at the two sides of a line.*

As illustrated in Fig. 1, Shapes 1, 2 and 3 are made of repeating a part, that is shown by red color, in sides of a regular polygon and shape 4 consists of repeating a part, in the same direction, on two sides of a line.

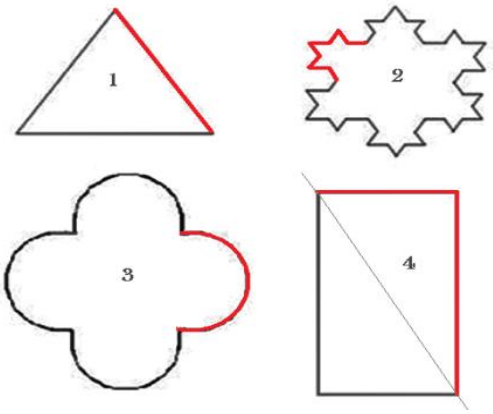

Fig. 1. Some regular shapes based on our definition

A similar definition for regular shape is proposed in the work of Gang wu et al. [4]: "A regular shape, such as a regular polygon or circle, possesses the characteristic that within the shape there is a point that has an equal distance to each side or the boundary of the shape". Their definition is limited to the polygon shapes. However, our definition has more generality and not only consists of polygon shapes but also non-polygon shapes such as shape 2. In addition, in the shapes 2 and 4 which are regular, based on our definition, we cannot find a point that has an equal distance to each side or the boundary of the shape. In the proceeding sections, based on our definition, we will propose a technique to find out whether a shape is regular or not.

3.0 DETECTION PROCEDURE

The detection process is concerned with the recognition level, but it is better to mention some of the pre-processing levels such as segmentation and representation that is essential for recognition level.

3.1. Segmentation

The first step is called image segmentation, or object isolation, in which each object, and its regions are isolated from the rest of the scene. Segmentation algorithms can conveniently be classified as *boundary-based* and *region-based* [5], [6], [7], [8]. *Boundary-based* algorithms detect object contours explicitly by using the discontinuity property, and *region-based* algorithms locate object areas explicitly according to the similarity property [7]. Some segmentation algorithms can be mentioned as follows: these two cases include the boundary-based group of methods: *Optimal edge detector* [9] and *watershed segmentation* [10], [11]. In the region-based method *multilevel thresholding technique* [12] and *region-growing technique* can be mentioned. Actually a miraculous segmentation

approach, which could segment all types of satellite images in an exact way, does not exist. Parameter selection and image thresholding plays an important role and have great influence on segmentation results due to its intuitive properties and the simplicity of the implementation [13] and the characteristic of the satellite images. It should be noted that, our method of detecting regular shape is totally dependent on image segmentation strategies of satellite images. Any appropriate approach for generating the segments of the regions on a satellite image could be employed. However, the method we apply in the segmentation part is relative and depends on the satellite image that we work on. The only important issue is that we should extract the signatures of the objects for image representation to find the local maxima that is explained in detail in the representation section. It should be noted that better segmentation leads to better results in differentiating between regular and irregular shapes.

3.2. Representations

The second step is called feature extraction where the objects are represented. A representation is the value of some quantifiable properties of an object. In this study, the segmented shapes are represented by their signatures [14]. A signature is a 1-D functional representation of a boundary. The simplest way of creating this function is to measure the distance of the boundary pixels from the centroid of the shape as the function of angle [14]. In Fig 2, the Signatures of some regular shapes are shown.

As can be seen, these signatures are composed of repeating M times of the first 1/M of the signature; where M is an integer. As demonstrated in Fig 2, the signature is the repetition of a part, which is shown with a red line for emphasis. It should be mentioned that the repeated part in the signature of a circle is its first point. Moreover, the equilateral triangle has 3 equal sides that have the same distance from its centroid. So, its signature has 3 equal parts as shown in Fig 2(b). The square also has 4 equal sides, and hence 4 repeated parts. As a result, in the shapes that have equal sides, the number of repeated parts is equal to the number of sides. However, as shown in Fig 2(d), in a rectangular that does not have equal sides, the two opposite sides are repeated, and consequently in its signature, each of the two adjacent non-equal parts make the repeated part.

3.3. Fourier representations

Here we present a subtle approach to achieve a suitable criterion to measure the amount of regularity in a shape. As mentioned in the previous section, the signature of a regular shape is composed of repeating M times of the first 1/M of the signature. Now, we try to inspect the property of the signature of a regular shape in Discrete Fourier Transform (DFT) domain. Assume a finite-length sequence $y[\mathrm{n}]$ is the signature of a regular shape which consists of repeating M times of the sequence $x[\mathrm{n}]$. Therefore the sequence $x[\mathrm{n}]$ is 1/M partition of the sequence $y[\mathrm{n}]$. $x[\mathrm{n}]$ is a finite-length real sequence. DFT of $x[\mathrm{n}]$ could be defined as follows [15]:

$$X[k] = \sum_{\mathrm{n}=0}^{\mathrm{N}-1} x[\mathrm{n}] W_{\mathrm{N}}^{k\mathrm{n}} \tag{1}$$

Where $W_{\mathrm{N}}^{k\mathrm{n}} = e^{-j\frac{2\pi}{\mathrm{N}}\mathrm{n}}$ and N is duration of the sequence $x[\mathrm{n}]$.

$y[\mathrm{n}]$ consists of repeating M times of $x[\mathrm{n}]$ so that, it can be written as below:

$$y[\mathrm{n}] = rep_{\mathrm{M}}(x[\mathrm{n}]) \tag{2}$$

The DFT of $y[\mathrm{n}]$ is:

$$Y[k] = \begin{cases} \mathrm{M}X[l] & for\ k = \mathrm{M}l \\ 0 & otherwise \end{cases} \tag{3}$$

$l = 0, 1, \ldots, \mathrm{N} - 1$

$$k = 0,1, \ldots, \mathrm{MN} - 1$$

Where the sequence $Y[k]$ is the DFT of the sequence $y[n]$. Further details and the proof of the above equations can be found in [16].

Based on Equation 3, the frequency indexes (k) of the nonzero elements are multiples of M. Hence, there exist M-1 zeros between each of the nonzero elements of $Y[k]$. *We use this striking property of the DFT of the signature representation of a regular shape as the key idea for inspecting regularity in arbitrary shape.* In other words, the periodic group of zeros in the frequency domain of a signature indicates the regularity of a shape and the number of zeros shows the number of the repeating parts (M). Furthermore, after implementing the DFT of the signature, we can search for the local maxima instead of periodic group of zeros in the frequency content to indicate regularity. If we have the intermittent local maxima, we can obtain the period M. For illustration, the signature representation of a rectangular and its DTF are demonstrated in Fig 3. As could be observed, DFT domain consists of periodic groups of zeros that occur between each of the nonzero elements.

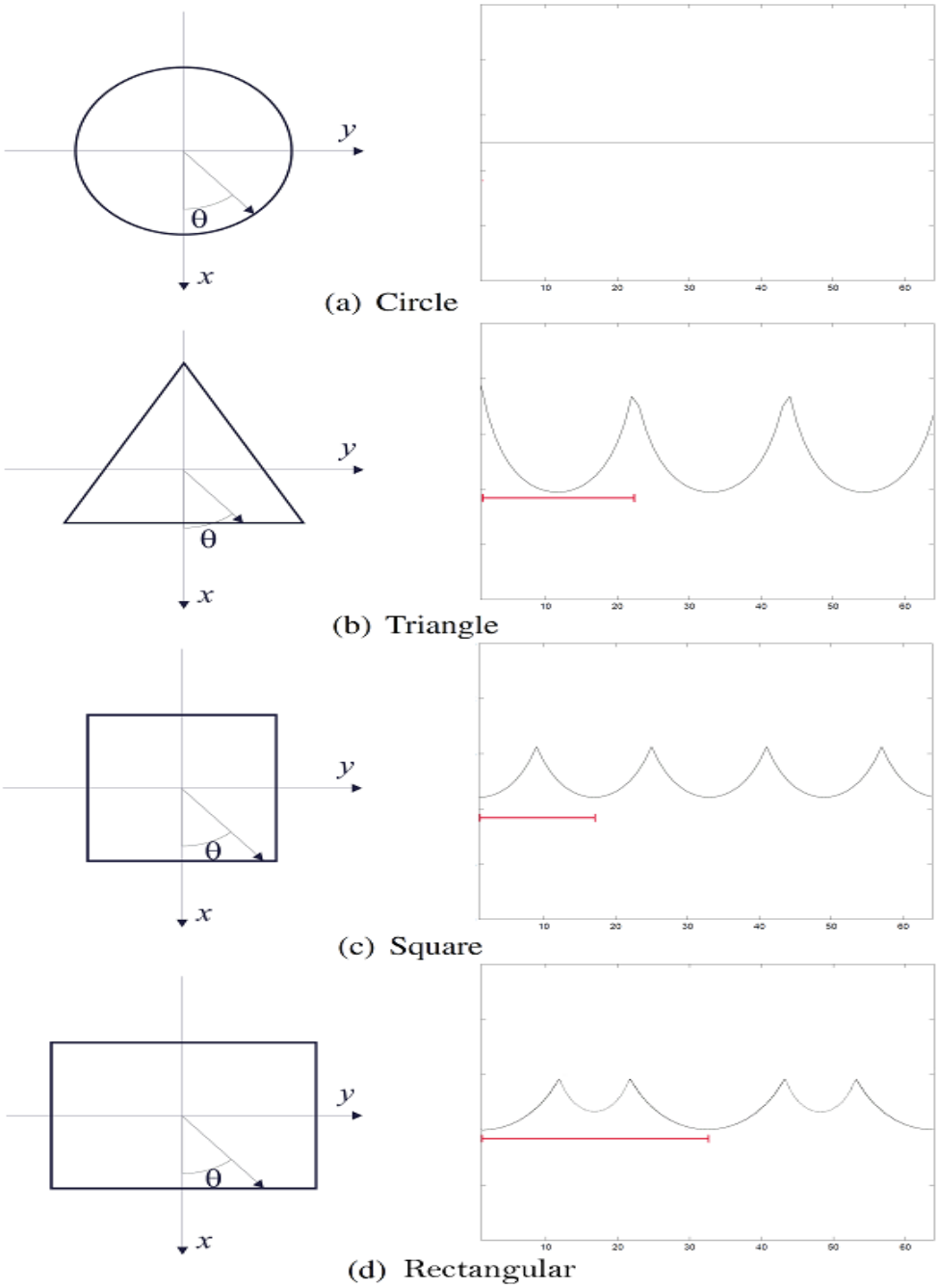

Fig. 2. Signatures of some regular shapes; the repeated part is depicted by red colour line, under the signatures

It should be mentioned that a similar study to our work has been done in the work of P. Gil et al. [17], which utilizes the Fast Fourier Transform (FFT) of the signature to distinguish regular road sign shapes. They compared the FFT of the signature of an extracted blob with the FFT of the signatures of the reference shapes, which were used for the classification of traffic sign shapes. In contrast to our work, their strategy is only capable of detecting regular polygon shapes that the FFT of their signatures are previously stored as reference data. Even though our technique applies the FFT of the signature, it uses an RCNR value, which is explained in the next section to distinguish regularity and do not need any reference data.

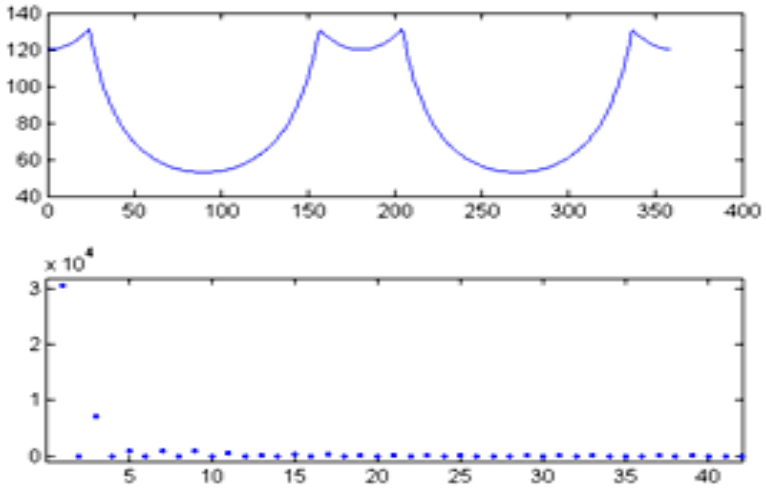

Fig. 3. Signature of a rectangular and its DFT; It is evident that zeros occurs with period M=2

3.4. RCNR Value

In practical point of view due to the restrictions in boundary sampling and noise, the signature of a regular shape is not exactly composed of the repetition of one part. In other words, there are some differences between the parts. Here, we model the differences by additive, uncorrelated zero mean noise. Consider $\hat{y}[\mathrm{n}]$ is the observed signature of a regular shape, which is contaminated by noise, Therefore the observed signature $\hat{y}[\mathrm{n}]$ is:

$$\hat{y}[\mathrm{n}] = y[\mathrm{n}] + n[\mathrm{n}] \tag{4}$$

Where $n[\mathrm{n}]$ denotes the additive noise and $y[\mathrm{n}]$ is the noise of the free signature. Taking DFT of $\hat{y}[\mathrm{n}]$ yields:

$$\hat{Y}[k] = Y[k] + N[k] \tag{5}$$

Where $\hat{Y}[k]$ and $N[k]$ are the DFT of $\hat{y}[\mathrm{n}]$ and $\hat{n}[\mathrm{n}]$ respectively. After taking DFT of $\hat{y}[\mathrm{n}]$, we look for the local maxima of the frequency contents. If the local maxima occur periodically, we can obtain the period M. Assume the period of the signature of $\hat{Y}[k]$ is M. Hence, the number of repeated parts in the signature of $\hat{y}[\mathrm{n}]$ is M. We divide $\hat{y}[\mathrm{n}]$ into M parts denoted by $\hat{y}_i[\mathrm{n}]$; Therefore, $\hat{y}[\mathrm{n}]$ and $n[\mathrm{n}]$ are also divided into M parts which are denoted by $y_i[\mathrm{n}]$ and $n_i[\mathrm{n}]$ respectively. Based on Equation 4:

$$\hat{y}_i[\mathrm{n}] = y_i[\mathrm{n}] + n_i[\mathrm{n}] \tag{6}$$

$$(i = 1, 2, \ldots, \mathrm{M})$$

Applying $\sum$ operator on both sides and then multiplying by $\frac{1}{\mathrm{M}}$ yield:

$$\frac{1}{M}\sum_{i=1}^{M} y_i[n] = \frac{1}{M}\sum_{i=1}^{M} \hat{y}_i[n] + \frac{1}{M}\sum_{i=1}^{M} n_i[n] \tag{7}$$

Now we define $x[n]$ as:

$$\hat{x}[n] \cong \frac{1}{M}\sum_{i=1}^{M} \hat{y}_i[n] \tag{8}$$

And assume:

$$y[n] = rep_M(x[n]) \tag{9}$$

Substituting of the Equation 9 and 8 into Equation 7 yields:

$$\hat{x}[n] = x[n] + \frac{1}{M}\sum_{i=1}^{M} n_i[n] \tag{10}$$

Now we compute statistical properties of $\hat{x}[n]$:

$$E\{\hat{x}[n]\} = E\{x[n]\} + \frac{1}{M}\sum_{i=1}^{M} E\{n_i[n]\} \tag{11}$$

We assume $n[n]$ has zero mean value, so:

$E\{n_i[n]\} = 0$, then:

$$E\{x\} = E\{\hat{x}\} \tag{12}$$

It is easy to show:

$$Var\{x\} = Var\{\hat{x}\} + \frac{1}{M}Var\{\hat{n}\} \tag{13}$$

It means that the effect of noise on $\hat{x}[n]$ is lesser than the effect of noise on $y[n]$. Therefore $x[n]$ tends to be similar to $\hat{x}[n]$:

$$x[n] \cong \hat{x}[n] \tag{14}$$

By using Equations 9 and 14 we can write:

$$y[n] \cong rep_M(\hat{x}[n]) \tag{15}$$

It is easy to approximate $n[n]$ by applying Equation 4 and 15. Now with these two values, we present a quantity that is named Reference Counter-to-Noise Ratio (RCNR) to evaluate the regularity in a shape:

$$\mathrm{RCNR} = 10log\left(\frac{S_{\hat{y}}}{S_{\hat{n}}}\right) \tag{16}$$

Where $S_{\hat{y}} = \sum_{n=0}^{MN-1}(\hat{y}[n])^2$ and $S_{\hat{n}} = \sum_{n=0}^{MN-1}(\hat{n}[n])^2$.

For regular shapes, whose signatures are exactly composed of the repetition of one part, the RCNR value should theoretically be an infinite value by the fact that there is no noise. However, in practical situation it has a finite value. Hence, one should assign a threshold value for RCNR to distinguish regular and irregular shapes.

As could be observed in the Fig 4, all the stages of inspecting the regularity in a satellite image could be explained as the following: after entering satellite image, we should segment the input image with an arbitrary approach to extract the foreground shapes from the background. A better segmentation approach, leads to a more precise regularity detection. The second preprocessing step is the signature extraction. After signature extraction, DFT representation of the signature should be implemented. That is a key idea for inspecting regularity due to the fact that the periodicity of the local maxima on the DFT domain of a signature indicates regularity. If there is no period for local maxima, then the shape is irregular. In the periodic case, the period shows that the shape could be divided into how many equal parts. Therefore, the repetition number (M), which is the number of equal parts, could be obtained. Then, we can compute $x[n]$ using Equation 14 and Equation 8. By repeating M times of $x[n]$, we can obtain $y[n]$ that is the estimated noise-free of the signature. By subtracting the original signature ($\hat{y}[n]$), which is contaminated by noise, from the estimated noise-free signature ($y[n]$), we can estimate noise ($n[n]$). Finally with these two values, we can compute the *RCNR* criterion that can be compared to a pre-assigned threshold value to inspect the regularity. In this case, if the computed *RCNR* value is higher than the threshold value, the shape is regular and if not, the shape is irregular. As depicted in Fig. 5, there are some regular and irregular shapes with their *RCNR* values. As can be seen, by assuming *RCNR*n as *RCNR* of the shape with index n, *RCNR*1=17.61, *RCNR*2=60.12, *RCNR*3=70.58, *RCNR*5=78.63. The shape 4 does not have periodic local maxima as shown in Fig. 5. In the shapes 3 and 5, RCNR value is high; hence we can conclude that these two shapes are regular. Shape 2 is quasi regular and its *RCNR* is lower than the shapes 3 and 5. The shape 1 is an irregular shape, but in frequency domain it has a periodic local maxima with low *RCNR* value. Shape 4 does not have a periodic local maxima; hence, it is not regular based on our definition. A threshold value for *RCNR* can be used to decide to some extent whether a shape is regular depending on the application.

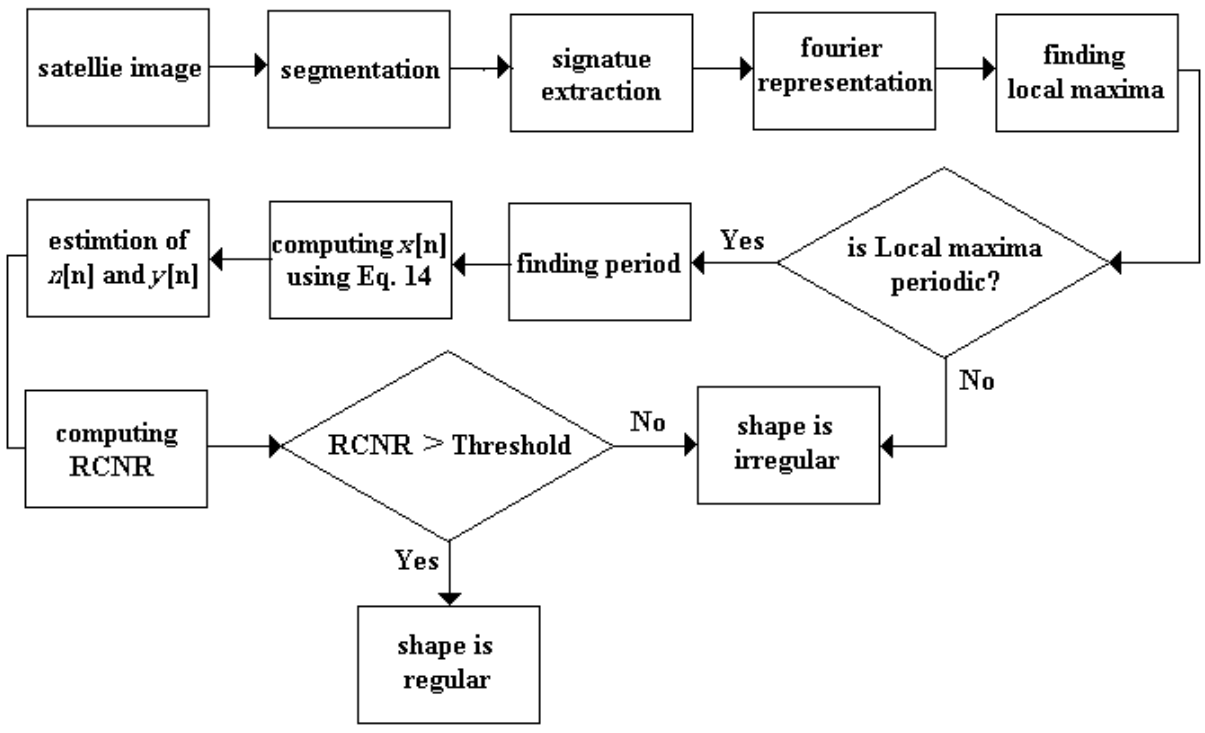

Fig. 4. The stages of the proposed method for inspecting the regularity of shapes in satellite images

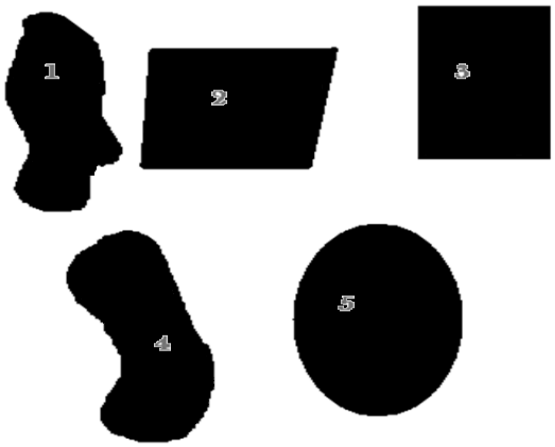

Fig. 5. Assume *RCNR*n is the RCNR of the shape with index n; *RCNR*1=17.61, *RCNR*2=60.12, *RCNR*3=70.58, *RCNR*4= *RCNR*5=78.63

3.5 Estimation of period

$y[n]$ is the signature of a shape and usually has low frequency contents. Consequently, it is enough to inspect the local maxima in the primary frequency bins (first 10 or 20 bins). Finding only 3 maximums are enough to estimate the repetition number (M). Here we suggest utilizing the chirp transform algorithm (CTA) [16] to compute the primary samples of the DFT.

3.6 Properties

Since representation by the signature of a boundary is robust against rotation and translation, it is apparent that *RCNR* is also robust against rotation and translation [14]. Fig. 6 illustrates robustness of *RCNR* value against the rotation and scale variation. Since shape 2 is the scaled and 90° rotated version of shape 1, their *RCNR* values are close to each other. The *RCNR* value of shape 1 is 78.56, which is close to the *RCNR* value of shape 2 that is equal to 82.68. Shape 4 is also a scaled and 90° rotated version of shape 3. The *RCNR* values of shapes 3 and 4 are 32.10 and 30.38 respectively. We can observe that these values are also close to each other. So, when a threshold value of *RCNR* is used for decision, we can say that this criterion has a good robustness against rotation and scale variation.

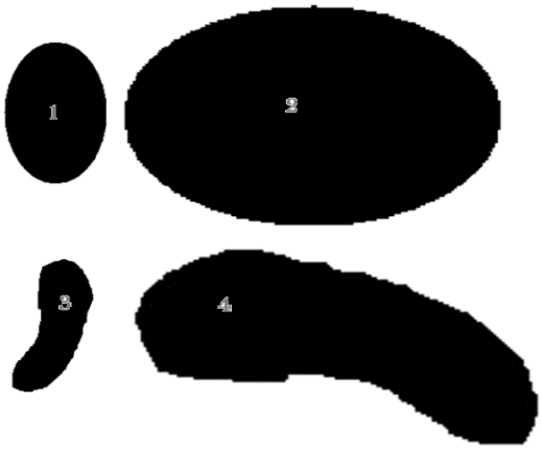

Fig 6. shapes 2 and 4 are scaled and 90° rotated version of shapes 1 and 3; *RCNR*1=78.56, *RCNR*2=82.68, *RCNR*3=32.10, *RCNR4*= 30.38

4.0 EXPERIMENTAL RESULT

In this section our purpose is to illustrate the performance of the proposed method for some samples of the real world to adjust the effectiveness of our proposed method. We have selected 3 different scenes of satellite images. The test images are gathered using *Google Earth software*. For all of the test images, global thresholding and morphological operation, is used to extract the foreground shapes from the background. Of course, any better segmentation method will lead to better results. Fig. 7(a) is an aerial image of an industrial factory. The result of classification by our method is depicted in Fig. 7(b). The red parts are the detected regular shapes based on our proposed strategy. The threshold value of *RCNR* for this test was considered as 30. As mentioned before, the threshold value of *RCNR* shows to some extent that a shape is regular. So the red parts shapes have the *RCNR* value above the considered threshold value. The value of *RCNR* depends totally on our application.

The results of implementing the proposed algorithm to another satellite image of a farm proved the capability of our algorithm in detecting regular shapes in satellite images. Figure 8(a) shows a farm satellite image and Figure 8(b) shows the classified image into two categories: regular and irregular. As could be observed, most of the shapes in this image are regular that is demonstrated with red colour and the white colour indicate the irregular parts. Therefore, most of the shapes have high *RCNR* values that indicate they have high regularity based on our definition. A threshold value of 60 was selected in this test.

Other testing samples are the satellite images extracted from a region in Japan. The images that are represented in Fig. 9(a) and Fig. 9(c), was taken before and after the disastrous tsunami (Japan, March 2011) respectively. As can be seen in Fig 9(c), most of the regular shapes have been destroyed due to tsunami. The number of regular shapes is fewer in this test in comparison with previous tests. Here, we classified the shapes based on two threshold values of 30 and 20 for *RCNR*. The detected regular shapes are shown with two different colours in Fig. 9(b) and Fig. 9(d). The red and green colours indicate the regular shapes using the threshold value of 30 and 20 respectively. In order to indicate the better conception of our algorithm, the *RCNR* values for some objects in this test are expressed. The numbers of 1, 2 and 3 that are demonstrated in Fig 9(b) and Fig 9(d) could specify three different shapes with different *RCNR* values. It is apparent that the regularity of these shapes is totally dependent on our threshold value. So, different threshold values can cause different categorization in the same image. In Fig 9(b), with a threshold value of 30, the shape with the *RCNR* value of 31.62, is considered regular (number 1). In Fig 9(d), with a threshold value of 20, the shape with the *RCNR* value of 25.23 is also regular (number 2). However, In Fig 9(b), with the threshold value of 30, the object with *RCNR* value of 24.13 is considered as irregular shape (number 3). This threshold value could be changed in another application. It should be noted that our segmentation method was a rudimentary approach. It is completely obvious that better segmentation methods could lead to better results.

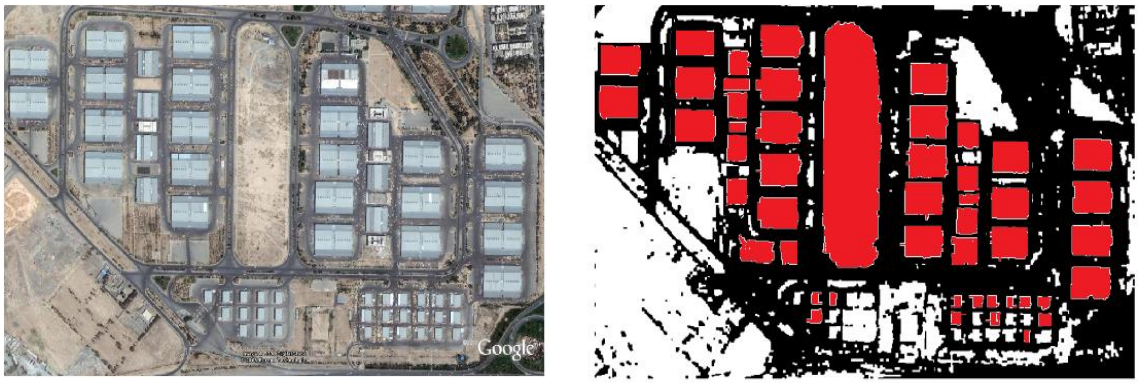

(a) (b)

Fig. 7. Aerial image of an industrial factory

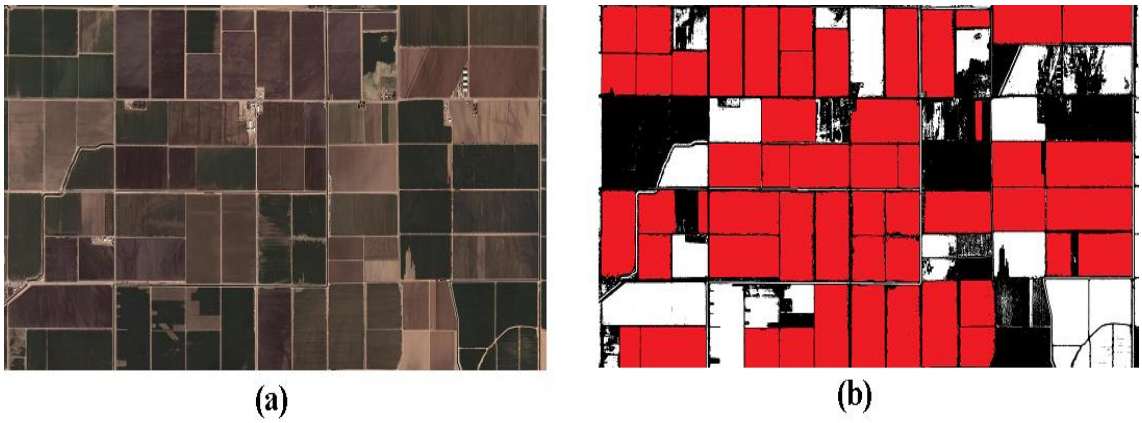

Fig. 8. Aerial image of a farm

5.0 CONCLUSION

In this study, we presented a novel and fast approach of detecting regular shapes in satellite images. First, we presented an appropriate definition of regular shapes that contains most of our objects of interest such as rectangular, square and circle. We used the significant property of the DFT of the signature representation of a regular shape as a key idea for inspecting regularity in an arbitrary shape. The periodicity of the local maxima in the DFT of a signature indicates regularity. One of the important problems is that the signature of a regular shape is not exactly composed of the repetition of one part. So, we should model the differences by additive noise. The period of local maxima has an important role in our procedure by the fact we can estimate one of the repeated parts in the noisy signature, and consequently the noise and noise-free signature could be evaluated. If there is no period for local maxima, then the shape is irregular. We presented a new criterion, that we named it *RCNR*. This criterion could distinguish to some extent that the shape is regular. The computed *RCNR* value should be compared with a pre-assigned threshold value for making decision. The *RCNR* value for irregular shapes is a low value, but it is relatively high in regular shapes. We can also use chirp transform algorithm in order to increase the computational speed. The proposed algorithm has a good robustness against rotation and scale variation and could be easily implemented. In addition, in contrast to the state of the art methods, our approach has a low processing time and it is independent of the shape. Experimental results proved that the proposed technique could be very effectively applied for satellite images and it could be employed in the variety of significant applications and further processing such as detecting man-made or artificial structures.

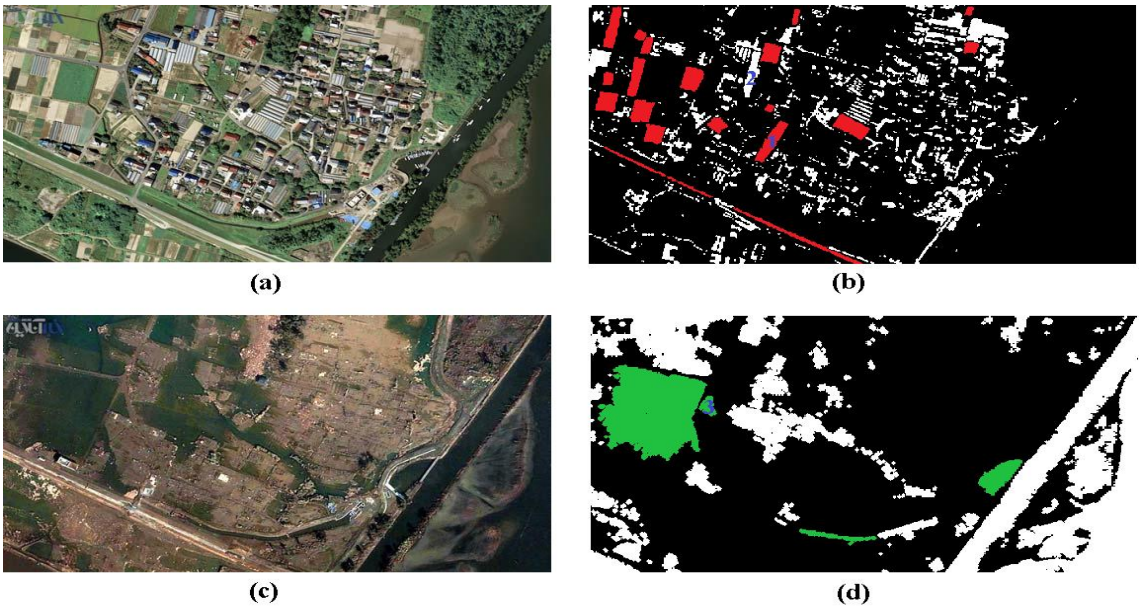

Fig 9. Aerial images of a location in Japan (March 2011). (a): before tsunami, (c): after tsunami

REFERENCES

[1] G. Piccioli, E. de Micheli, P. Parodi and M. Campani, "Robust Method for Road Sign Detection and Recognition", *Image and Vision Computing*, Vol. 14, 1996.

[2] N. Barnes, G. Loy, D. Shaw and A. Robles-Kelly, "Regular polygon detection", *IEEE InternationalConference on Computer Vision*, 2005.

[3] A.de.L. Escalera, L.E. Moreno, M.A. Salichs and J.M. Armingol, "Road Traffic Sign Detection and Classification", *IEEE Transactions on Industrial Electronics*, Vol. 44, No. 6, 1997.

[4] G. Wu, W. Liu, X. Xie, Q. Wei: "A Shape Detection Method Based on the Radial Symmetry Nature and Direction-Discriminated Voting". *ICIP (6)* 2007, pp169-172.

[5] B. Nicolin, R. Gabler, "A knowledge-based system for the analysis of aerial images, *IEEE Transaction on Geoscience and Remote Sensing*.Vol 25, No. 3, 1987,1987, pp 317-329.

[6] B.Guindon, "Computer-based aerial image understanding: A review and assessment of its application to planimetric information extraction from very high resolution satellite images", *Canadian Remote Sensing*, Vol. 23, No. 1, 1997, pp 38-47.

[7] Y.J. Zhang, "Evaluation and comparison of different segmentation algorithms, *Pattern Recognition Letters*, Vol. 18, 1997, pp 963-974.

[8] L.L.F, Janssen, and M. Molenaar, "Terrain objects, their dynamics and their monitoring by the integration of GIS and remote sensing", *IEEE Transaction on Geoscience and Remote Sensing*, Vol. 33, No. 3, 1995, pp 749-75.

[9] J.Canny,"A computational approach to edge detection, *IEEE Transactions on Pattern Analysis and Machine Intelligence*, PAMI-8, 6,1986, pp679-698.

[10] L.Vincet, P. Soille, "Watershed in digital spaces: An efficient algorithm based on immersion simulations", *IEEE Transactions on Pattern Analysis and Machine Intelligence*, Vol. 13, No. 6, 1991,pp 583-598.

[11] O. Debeir, "*Segmentation supervisee d'Images*, Ph.D., Faculte' des Sciences Applique'es, Universite' Libre de Bruxelles, 2001.

[12] F. Deravi, and S.K. Pal, "Grey level thresholding using second-order statistics", *Pattern Recognition Letters*, Vol. 1, 1983, pp 417-422

[13] R.C. Gonzalez, R. E. Woods, "*Digital Image Processing 2nd Ed*", Prentice Hall Inc, 2002, pp 595-596.

[14] R.C. Gonzalez, R.E. Woods, "*Digital Image Processing 2nd Ed*", Prentice Hall Inc, 2002, pp 643-692.

[15] A.V. Oppenheim, R.W. Schafer, J.R. Buck, "*Discrete-Time Signal Processing*" (2nd Edition) (Prentice-Hall Signal Processing Series).

[16] A.V. Oppenheim, R. W. Schafer, J. R. Buck. "*Discrete-Time Signal Processing*" (2nd Edition) (Prentice-Hall Signal Processing Series) chirp transform alghorithm(CTA), pp656-61.

[17] P. G. Jimenez, S. L. Arroyo, H. G. Moreno, F.L. Ferreras and S. M. Bascon, "Traffic Sign ShapeClassification Evaluation II: FFT Applied to the Signature of Blobs", *IEEE Intelligent Vehicles Symposium*, 2005.

[18] G. Gallo, G. Grasso, S. Nicotra, A. Pulvirenti, "Remote sensed images segmentation through shape refinement".*11th International Conference on Image Analysis*, 6-28 September 2001, pp: 137 –144.

[19] R. M. Hadad, P. P. Martins Jr., A.D. A. Araújo: Using the Hough Transform to Detect Circular Forms in Satellite Imagery. *SIBGRAPI* 2001: 406.